

DESIGN NOTE

The development of a low-cost focusing probe for profile measurement

K C Fan[†]§, C Y Lin[†]|| and L H Shyu[‡]¶

[†] Department of Mechanical Engineering, National Taiwan University, Taipei, Taiwan, Republic of China

[‡] Department of Electro-Optics Engineering, National Huwei Institute of Technology, Huwei, Taiwan, Republic of China

E-mail: fan@ccms.ntu.edu.tw

Received 8 July 1999, in final form 14 September 1999, accepted for publication 21 September 1999

Abstract. A high-precision optical probe based on the principle of focusing-range detection is developed in this research. The probe adopted for use was directly taken from the pick-up head of a CD player. Because its principle is similar to that of the autofocusing probe, the characteristics of each component of the head were investigated and its conversion into a focusing probe was attempted. The S-curve within the focusing range can be analysed, revealing the linear relationship between the normalized focus-error signal (FES) and the measured distance. The system accuracy of the probe was found. Within the measurement range of 10 μm the linearity error was about 1%, the standard deviation was about 34 nm and the frequency response was about 8 kHz. Some practical applications were carried out, namely profile measurements of a step height, a CD surface and a silicon-wafer grating. All results were highly consistent with the nominal values.

Keywords: CD pick-up head, focusing probe, focus error, precision measurement

1. Introduction

Technologies of ultra-precision machining have grown rapidly in recent years. The corresponding inspection technologies with both resolution and accuracy in the submicrometre or even nanometre range have also received great attention worldwide. Most researchers, however, have devoted their efforts to developing sophisticated and expensive systems such as STM [1], AFM [2], confocal probes [3] and autofocusing probes [4]. Although these systems are very useful in ultra-precision profile measurements, they can be employed only by organizations having sufficient budgets, such as the famous Molecular Measuring Machine (MMM) project which has been being developed by the NIST since 1988 [5]. Some mature laser technologies in precision measurement can be categorized in principle into the following categories: (i) triangulation method [6, 7], (ii) autofocusing methods [4, 8], (iii) confocal methods [3], (iv) scattering methods [9, 10] and (v) heterodyne interferometric methods [11–14].

§ Professor.

|| Graduate student.

¶ Associate professor.

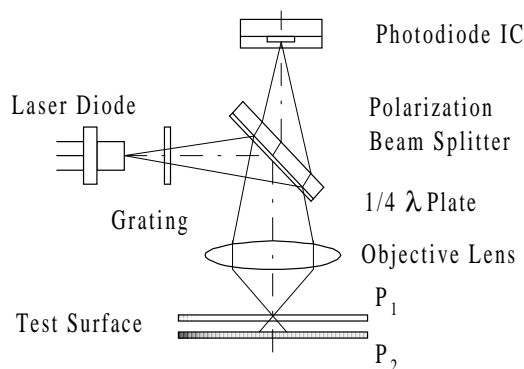


Figure 1. The focusing-measurement principle.

The success of compact-disc technology is based on the development of highly sophisticated, compact and inexpensive pick-up heads, which have provided a basis for many applications such as position measurements [15] and angle measurements [16]. A three-dimensional profilometer utilizing the 'in-focus' signal of a CD-player reading head was developed for contact-lens measurement [17].

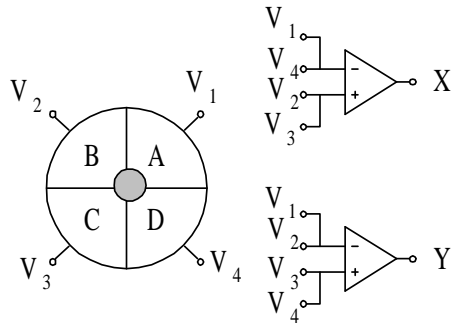


Figure 2. The four-quadrant detector.

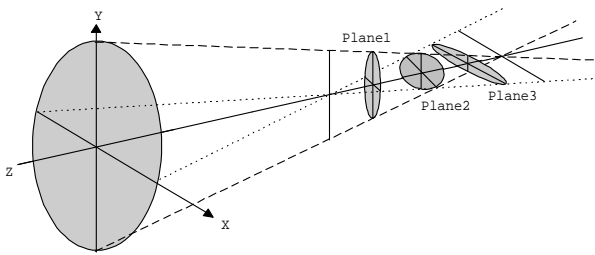


Figure 3. The principle of the astigmatic method.

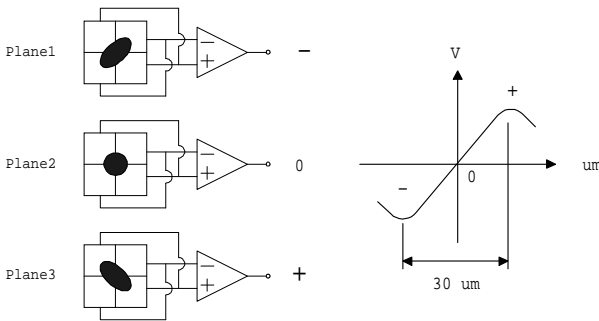


Figure 4. The variation of the spot shape with distance producing an S-curve of the FES.

This research was intended to develop a low-cost optical probe with measurement capability in the submicrometre range. The pick-up head of the commercial CD player was adopted for use on the basis of its principle of focus error. By appropriate modification of its signal processing unit, this head can be converted into a profile probe with submicrometre accuracy. In principle, instead of using the ‘in-focus’ signal, this research directly output the analogue S-curve signal, which also made fast measurement possible.

2. The principle of the measurement

A pick-up head was taken from a commercial CD player (SONY CXA1753M, with numerical aperture (NA) 0.45, wavelength 780 nm and depth of focus $\pm 2.3 \mu\text{m}$ [18]). In principle, it is an autofocusing laser probe, as shown in figure 1. Light from a laser diode is first polarized by a grating plate. Having passed through a beam splitter and a quarter-wave plate (mounted on the beam splitter), it is focused by an objective lens onto the object surface as a spot approximately $1 \mu\text{m}$ in diameter, about 2 mm from the sensor. The reflected beam signal is imaged onto a four-quadrant photodetector within the sensor by means of the quarter-wave plate. The photodiode outputs are combined to give a focus-error signal (FES) which is used to control the position of a movable lens within the sensor such that the focal spot of the beam remains coincident with the object surface. It should be noted here that, in the original structure of the pick-up head, the objective lens is suspended by a voice-coil motor. The lens will be actuated to vary its position dynamically in order to track the disc in focus when the fly height changes. Because in this research we are interested only in the signals within a fixed focusing range, the voice-coil motor was therefore purposely glued so as to be inactive, yielding a focusing probe. This is why the voice-coil motor is not shown in figure 1. Experimental tests showed that, with an adhesive epoxy resin, the objective lens could be fixed steadily with only 25 nm variation [19]. The FES is defined here as

$$\text{FES} = (V_1 + V_3) - (V_2 + V_4) \quad (1)$$

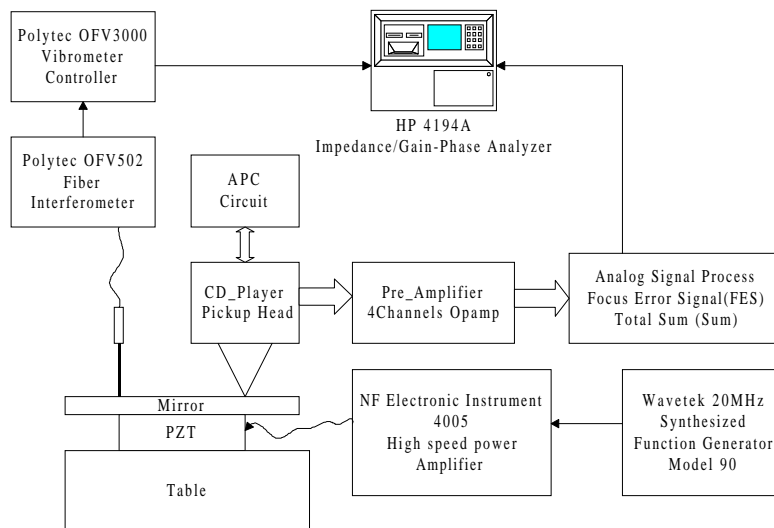
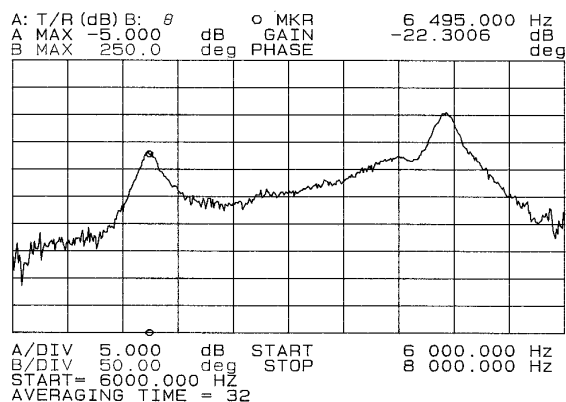
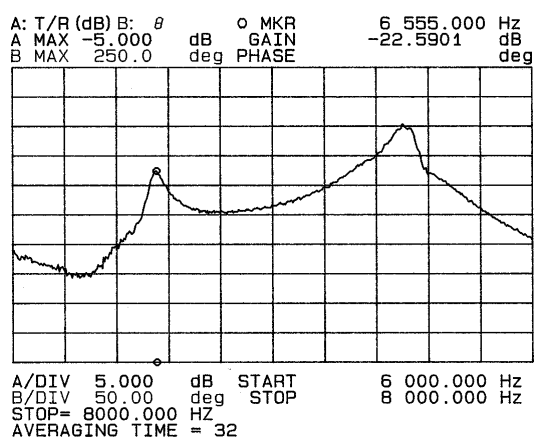


Figure 5. The system diagram of the dynamic-performance test.



(a)



(b)

Figure 6. Tested spectrum diagrams with (a) the interferometer and (b) the focusing probe.

where V_1 , V_2 , V_3 and V_4 are the output voltages of the quadrant detectors A, B, C and D respectively, shown in figure 2.

In this system, the focusing signal is detected by the astigmatic method, as shown in figure 3. At the focal plane, the spot is a pure circle, whereas, away from the focal plane,

the spot appears an elliptical shape in various orientations inside or outside the focal planes. The light pattern is then detected by the photodiode to produce a FES, which outputs an S-curve proportional to the distance, as shown in figure 4. The linear range can be found to be about $30 \mu\text{m}$ and this is the measuring range we can use to detect a change in the profile of the object surface. The output power of the laser diode is very sensitive to the ambient temperature. An automatic power-control (APC) circuit is usually employed to stabilize the output power via a feedback signal from the power monitor. In this work, an APC circuit was designed to monitor and control the driving power of the laser diode through a power detector and a reference voltage. It was found that, with an APC circuit, the variation of the input voltage of the laser diode could be maintained within $\pm 0.03 \text{ V}$ during a 4 h run. In comparison with 0.6 V drift with a normal power supply under the same test conditions, the use of an APC circuit in this system is significant.

3. Calibration of the system

3.1. The dynamic performance

Figure 5 shows the experimental set-up for testing the dynamic performance. A piezoelectric transducer (made by Physik Instrumente with nominal expansion $10 \mu\text{m}$ at 100 V) was actuated to provide fast dynamic motion with a stroke of $0.2 \mu\text{m}$. A fibre interferometer (made by Polytec Co, model QFV 502) was used as a reference to compare with the output response of the investigated pick-up head. Both signals were analysed by the HP 4194 FFT. Figures 6 shows the spectrum diagrams of both signals, from which we can find that the frequency response of the pick-up head can reach 8 kHz without distortion. The maximum dynamic response was estimated to be about 10 kHz.

3.2. The S-curve-performance test

In the profile measurement of ultra-fine surfaces, we are interested in the characteristics of the S-curve with respect

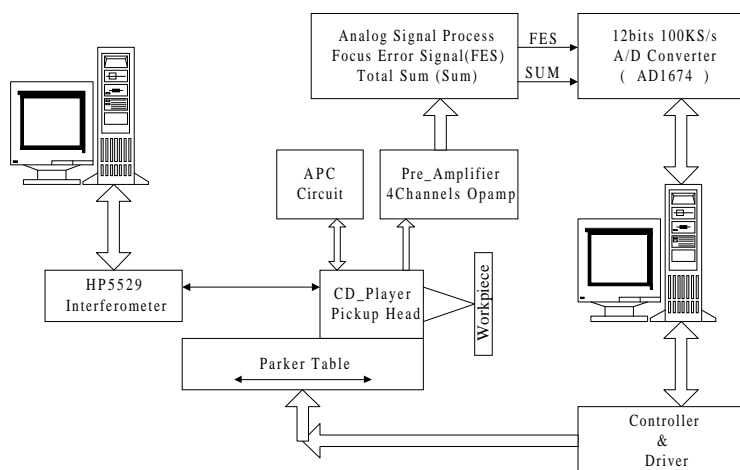


Figure 7. The set-up for the S-curve test.

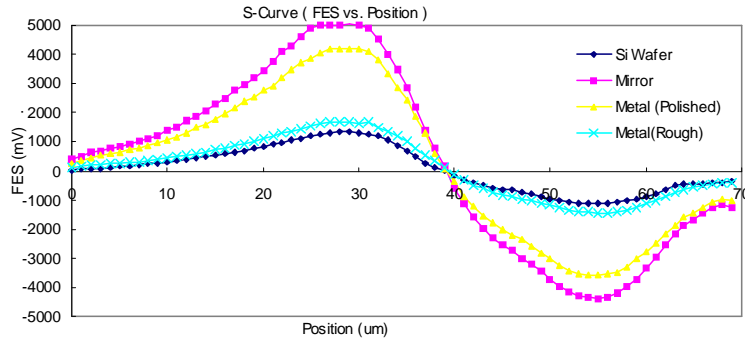


Figure 8. S-curves for various materials.

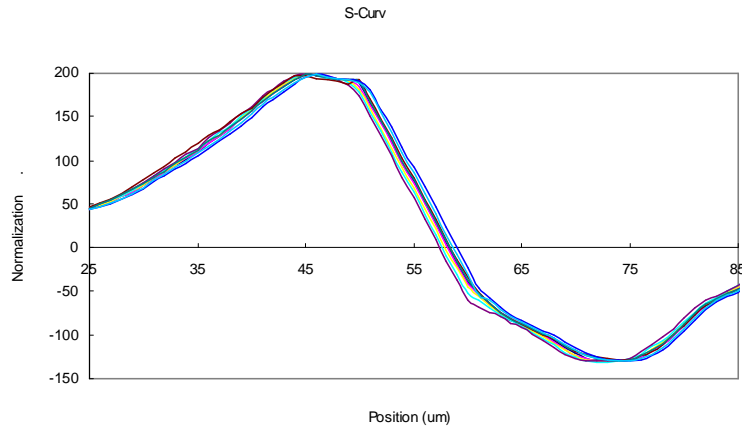


Figure 9. The reproducibility of the S-curve for a particular material.

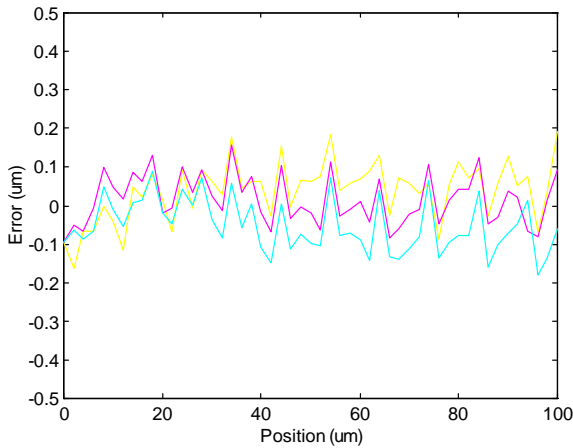


Figure 10. The compensated positional error due to the motor mechanism.

to the test surface. Figure 7 shows the set-up for the S-curve calibration. The object was fixed and the pick-up head was driven by a micro-positioning stage, made by Parker Co. The displacement of the stage was detected by a HP 5529 laser interferometer whose readout was plotted against the FES of the pick-up head. Figure 8 shows that different object materials, due to their different reflectivities, may produce different S-curves. Such a phenomenon is reasonable in that the better the surface roughness the steeper the S-curve. The reproducibility of the S-curve for a particular material was

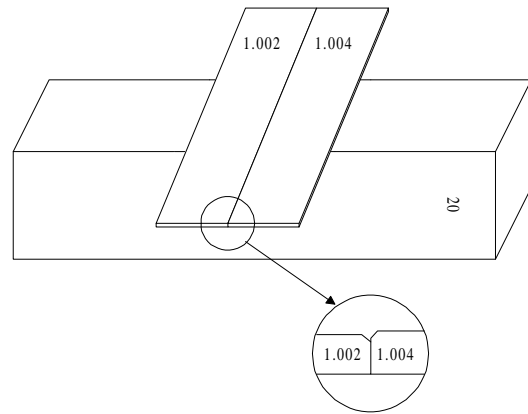


Figure 11. The arrangement of two gauge blocks.

also investigated. It was found that only with the normalized FES, i.e. the measured FES divided by the sum of the signal intensity, could the S-curve remain highly reproducible. A typical example for a polished metal surface is given in figure 9. From figure 9, if we select the linear range as $10 \mu\text{m}$ (from $50 \mu\text{m}$ to $60 \mu\text{m}$ of the position), statistical results of nine runs show that the averaged linearity error is about 1% and the mean standard deviation is 33.9 nm . The linearity error for each run is defined as

$$\text{linearity error} = \frac{\text{(maximum residual of fitted line)}}{\text{(linear range)}} \quad (2)$$

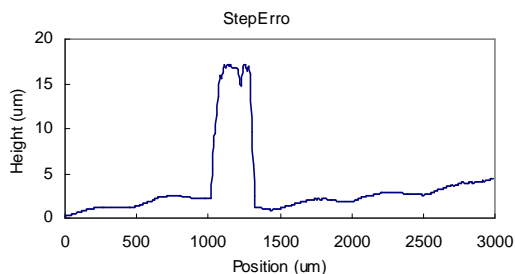


Figure 12. The measured signal for the step height.

Another investigation that we performed concerned the effect of the slope of the tested surface. It was also found that, within $\pm 2.5^\circ$ variation in slope angle of the tested surface, the standard deviation of the S-curve's slope is 0.205. This is regarded as the acceptable range for the slope of the tested surface.

4. Experimental results

Three cases were examined in this study, namely the step height of gauge blocks, the surface profile of a CD and the

grating on the surface of a silicon wafer. The probe was carried by a linear stage in such a way as to move across the object surface in incremental steps.

4.1. The positioning accuracy of the linear stage

Just like with all precision-measurement instruments, the motion accuracy of the probe carrier should also be verified for the profile measurements. This research employed a low-cost precision micro-position stage made by Parker Co. A preliminary calibration of the positioning accuracy of this stage was carried out using the HP 5529 laser interferometer [20]. From experiments, two types of pitch errors for a microstage investigation were found and their causes analysed. Model simulations of error were derived and feed-forward compensation schemes were implemented respectively. It was found that the feed mechanism could resolve the cyclical errors of larger pitches and motor-mechanism yields for cyclical errors of smaller pitch. By compensating for the mechanical errors, the positional accuracy could be enhanced from ± 2.5 to $\pm 0.5 \mu\text{m}$. Moreover, with the implementation of fine pitch-error compensation, the final accuracy could be further enhanced

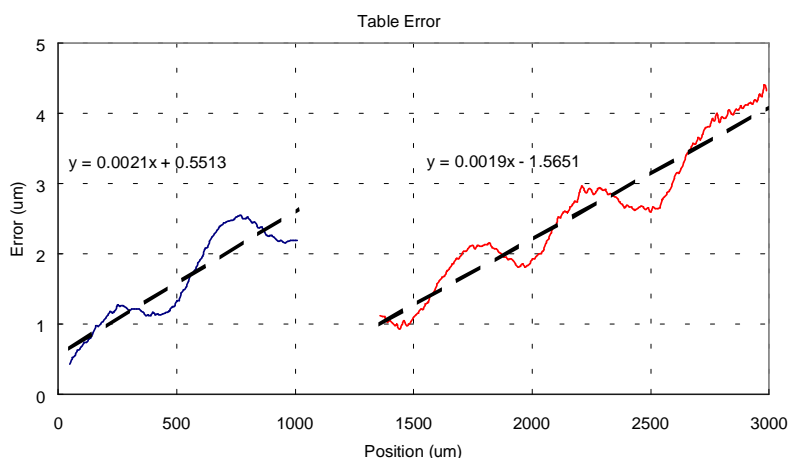


Figure 13. Results after filtering and line fitting.

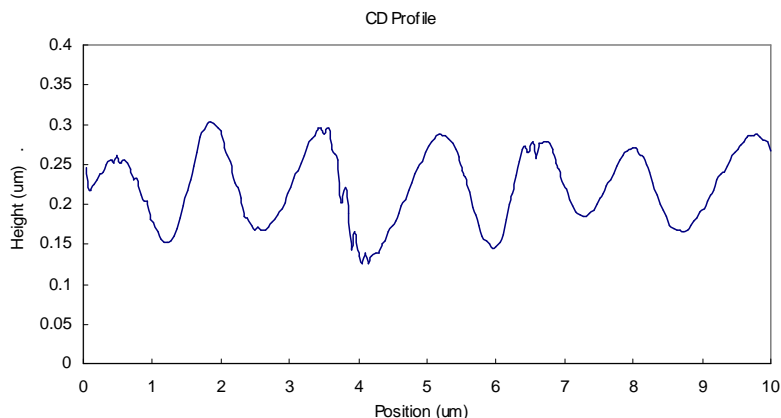


Figure 14. The measured CD profile.

Design note

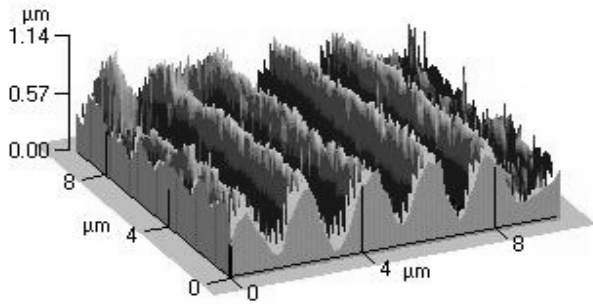


Figure 15. The gratings on a wafer measured by use of an AFM.

from 0.6 to $\pm 0.1 \mu\text{m}$, as shown in figure 10. A significant improvement in the positional control of the microstage was achieved.

4.2. The step height of gauge blocks

Two grade-one gauge blocks with nominal lengths of 1.004 and 1.002 mm respectively were put together on a reference plane, as shown in figure 11. The focusing probe scanned the surface across the step height. Received signals were dramatically influenced by the chamfer of each block, which reflected the light away from the sensor. The sum of light intensity accordingly dropped and hence the FES jumped up, as shown in figure 12. Using the least-squares method, two straight lines can be fitted to two sides of surface data respectively, as shown in figure 13. The distance of the offsets of these two straight lines (0.5513 and -1.5651) was found to be about $2.11 \mu\text{m}$, which is very close to the nominal value.

It was also found from this example that the sinusoidal waviness imposed on the measured profile was entirely caused by the waviness error of the linear stage because its wavelength was exactly the same as the pitch of the stage. Because its amplitude will be superimposed on the surface data in profile measurements of the following two applications, a simple sinusoidal function with amplitude $0.35 \mu\text{m}$ and pitch $0.5 \mu\text{m}$ was employed to represent the waviness error of the stage, which will be subtracted from the measured data.

4.3. The surface profile of a CD

From the specifications given by the manufacturer, the track distance of the investigated CD is $1.5 \mu\text{m}$ and the height is $0.2 \mu\text{m}$. Using a precision microstage, with feed-forward compensation of its calibrated positioning error to drive the focusing probe and with compensation of the measured data for waviness error, the surface profile can be obtained as shown in figure 14. It was found that the measured track distance was around $1.4\text{--}1.7 \mu\text{m}$ and the peak-to-valley distance was $0.15 \mu\text{m}$ on average. The errors could be due to the uneven etched depth of the CD and the spot size of the laser beam ($1 \mu\text{m}$). However, the deviation was not too bad.

4.4. The grating of a silicon wafer

A silicon wafer was coated with photoresist and gratings were etched into it. Its surface profile was first measured by using an AFM, with results as shown in figure 15. Compared with the profile measured by the developed system, plotted in figure 16, the scale height of $1 \mu\text{m}$ and the intergrating space of $2 \mu\text{m}$ are all quite consistent. It is proved that the developed system has an accuracy level similar to that of the commercial AFM.

An interesting phenomenon is found from this and the previous examples, namely that, even with a higher slope than expected, the surface profile can still be detected. It is true that, for a mirror surface, as used in the tilt-effect test in section 3.2, the light will be deflected if the slope is large. However, both the investigated grating samples have obvious roughness, which can scatter some of the light back to the photodetector. The normalized FES is essentially insensitive to the intensity of the light received. In addition, the spot size is about $1 \mu\text{m}$ in diameter, which projects an area beam, rather than an infinitesimal beam, onto the surface. From this study, it is also realized that the principle of the focusing probe observes the law of light scattering. The received signals refer to the mean changes of height of the projected area.

5. Concluding remarks

Optical probing has become more and more important for precision profile measurements in recent years. Although

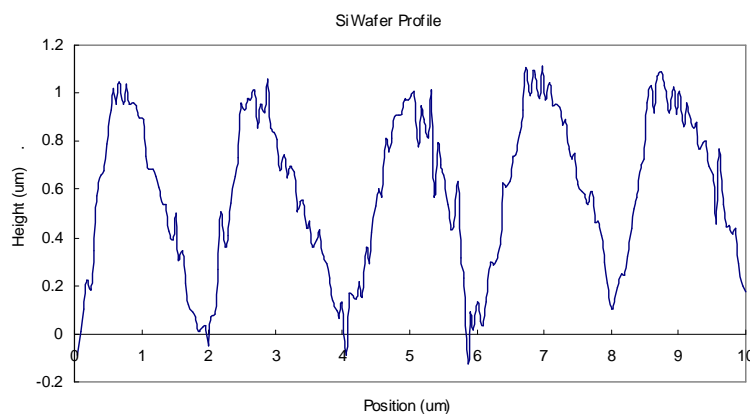


Figure 16. The gratings on a wafer measured by this system.

some autofocusing measurement systems can be found on the market, the prices are normally extremely high, say, of the order of £20 000. In this research we directly adopted for use a low-cost pick-up head from a CD player and developed our own signal processor. The voice-coil motor of the pick-up head was glued so as to be inactive, yielding a focusing probe. Using the linear range of the S-curve, the optical probe developed could satisfy the following specifications

- (i) The system linearity error is about 1% with standard deviation 34 nm.
- (ii) The measuring range is 10 μm .
- (iii) The bandwidth is at least 8 kHz.

Other useful items of information are worth pointing out here; namely that the carrying stage should be calibrated for its positioning error and waviness error before use and that the focusing probe observes the law of light scattering. The focusing-probe system developed can be used not only for high-precision profile measurements but also possibly for dynamic or microvibration measurements. In future we will try to attain a larger measuring range for which the whole autofocusing function of the pick-up head will be fully utilized.

Acknowledgments

The authors wish to express their gratitude towards the National Science Council of the ROC which sponsored this research through a project called 'Development of Nano-CMM'.

References

- [1] Akamine S, Albrecht T R, Zdeblick M J and Quate C F 1989 Microfabricated scanning tunneling microscope *IEEE Electron Device Lett.* **10** 490–2
- [2] Binning G, Quate C F and Gerber C H 1986 Atomic force microscopy *Phys. Rev. Lett.* **56** 930–3
- [3] Deng K L and Wang J P 1994 Nanometer-resolution distance measurement with non-interferometer method *Appl. Opt.* **33** 113–16
- [4] Yu H, Xie X B and Liu X J 1997 Measuring in surface roughness *Proc. APSI'97, China* pp 64–6
- [5] Kramer J, Penzes W, Scire F, Teague C, Villarrubia J, Amatucci E and Gilsinn D 1999 The molecular measuring machine *Proc. ICMT, Taiwan* pp 477–87
- [6] Mashimo K Nakamura T and Tanimura Y 1997 Development of optical noncontact sensor for measurement of three-dimensional profiles using depolarized components of scattered light *Opt. Eng.* **36** 227–34
- [7] Cheng L and Siu G G 1990 Measurement of surface roughness with core-ring ratio method using incoherent light *Meas. Sci. Technol.* **1** 1149–55
- [8] Zhang J H and Cai L L 1997 An autofocusing measurement system with piezoelectric translator *IEEE/ASME Trans. Mechatronics* **2** 213–16
- [9] Takahashi S, Miyoshi T and Takaya Y 1996 Study on nano-inprocess measurement of silicon wafer surface defects by laser scattered defect pattern *Proc. ISMTII'96, Tokyo* pp 243–50
- [10] Persson U 1996 Measurement of surface roughness using infrared scattering *Measurement* **18** 109–16
- [11] Makosch G and Drollinger B 1984 Surface profile measurement with scanning differential ac interferometer *Appl. Opt.* **23** 4544–53
- [12] Oh K J, Zhang Z H and Kim D W 1997 Measurement of rough surface profile using multiport homodyne interferometer *Proc. APSI'97, China* pp 164–6
- [13] Hillmann W, Brand U and Krystek M 1996 Capabilities and limitations of interference microscopy for two- and three-dimensional surface measuring technology *Measurement* **19** 95–102
- [14] Yu Y J, Li P S, Yu Y M and Zhang Z 1997 The effect of lateral resolution on surface roughness measurement in the heterodyne interferometer *Proc. APSI'97, China* pp 282–5
- [15] During C, Anderson S and Wilkander J 1992 Non-contact absolute measurement using a compact disc player optical pick-up *Sensors Actuators A* **32** 575–81
- [16] Armstrong T R and Fitzgerald M P 1992 An autocollimator based on the laser head of a compact disc player *Meas. Sci. Technol.* **3** 1072–6
- [17] Ehrmann K, Ho A and Schindhelm K A 1998 A 3D optical profilometer using a compact disc reading head *Meas. Sci. Technol.* **9** 1259–65
- [18] Sony Co 1997 Photo Device CXA 1753M *SONY semiconductor product list 1997:4* p 55
- [19] Lin C Y 1998 Development of an ultra precision laser focusing probe *MS Thesis* National Taiwan University
- [20] Fan K C, Lin C Y and Shyu L H 1998 Positional error compensation of a precision microstage *J. CSME* **19** 543–8